Electronic Supplementary Material (ESI) for New Journal of Chemistry.

Electronic Supplementary Information

Cysteine-based silver nanoparticles as dual colorimetric sensors for cations and anions

P. P. Praveen Kumar, Lakshay Kathuria and V. Haridas *

Department of Chemistry, Indian Institute of Technology Delhi, New Delhi -110016, India

*Corresponding author: Tel.: +91 011 2659 1380; e-mail address: haridasv@iitd.ac.in.

General experimental section

All solvents employed in the reactions were distilled and dried prior to use. Compounds were purified by silica gel column chromatography (silica gel 60-120 mesh) using either hexane/ethyl acetate or chloroform/methanol as eluents. Thin-layer chromatography (TLC) using Silica gel G (Merck) was used for monitoring the reaction. NMR spectra were recorded on Brucker-DPX-300 (^{1}H, 300 MHz; ^{13}C, 75 MHz) spectrometer using tetramethylsilane (^{1}H) as an internal standard. Coupling constants are in Hz and the ^{1}H NMR data are reported as s (singlet), d (doublet), br (broad), br d (broad doublet), t (triplet), m (multiplet). IR spectra were recorded on a Nicolet, Protégé 460 spectrometer and the samples were made as KBr pellets. Melting points were recorded on a Fisher-Johns melting point apparatus and were uncorrected. Bruker MicrO-TOF-QII model spectrometer was used for High Resolution Mass Spectra (HRMS) measurements. UV-visible spectra were recorded in Shimadzu double beam spectrophotometer, UV-2400 with 1 cm quartz cell. HR-TEM was recorded on TECHNAI G2 (20STWIN) electron microscope. Dynamic light scattering experiment was performed using Malvern Zetasizer ZS90 DLS spectrometer with 633 nm CW laser. EDX-SEM experiments were performed by ZEISS EVO®18 instrument with an EHT of 20 kV.

Preparation of 3a

To a solution of compound **2** (100 mg, 0.22 mmol) in dry acetonitrile, diisopropylethylamine (DIEA) (0.083 ml; 0.48 mmol) was added. After 5 minutes, p-nitrophenyl azide (79.37 mg, 0.48 mmol) and CuI (9.14 mg, 0.09 mmol) were added and the reaction mixture was kept stirred for 24 h. The solvent was removed under reduced pressure and the reaction mixture was redissolved in CH_2Cl_2 and washed sequentially with 9:1 NH_4Cl/NH_4OH solution, 0.2 N H_2SO_4, saturated $NaHCO_3$ solution and finally with water. The organic layer was dried over Na_2SO_4, evaporated and purified by column chromatography using $CHCl_3/MeOH$ as eluents to yield 79 mg of **3a**.

Yield: 46 %

m.p : 218-220 ^{o}C

^1H NMR ($CDCl_3$, 300 MHz) δ: 1.42 (s, 18 H), 2.95 (m, 4 H), 4.61 (m, 2H), 4.69 (m, 2H), 4.90 (br s, 2H), 5.53 (d, *J* = 9.6 Hz, 2H), 7.96 (d, , *J* = 9 Hz, 4 H), 8.13 (s, 2H), 8.41 (d, *J* = 9 Hz, 6H).

^{13}C NMR ($CDCl_3$, 75 MHz) δ: 28.3, 34.9, 46.7, 54.5, 80.7, 120.3, 120.6, 125.5, 141.0, 146.2, 147.1, 155.9, 170.7.

IR (KBr) : 3344, 2978, 2930, 1666, 1602, 1526, 1345, 1251 cm^{-1}

HRMS : Calculated for $C_{34}H_{42}N_{12}O_{10}S_2Na$ m/z : 865.2486, obtained 865.2460

Preparation of 3b

To an ice cooled solution of **3a** (100 mg, 0.11 mmol) in dry CH_2Cl_2, trifuloroacetic acid (TFA) (0.36 ml, 4.75 mmol) was added. After completion of reaction as monitored by TLC, the reaction mixture was subjected to high vacuum and redissolved in ethyl acetate and washed with 10% aq. Na_2CO_3 solution. The organic layer was dried over Na_2SO_4, evaporated and precipitated by diethyl ether to yield 70 mg of **3b**.

Yield: 92 %

m.p : 156-158 °C

^{1}H NMR (D_2O, 300 MHz) δ: 3.05 (m, 2H), 3.18 (m, 2H), 4.15 (br s, 4H), 4.36 (br s, 2H), 7.35 (d, *J* = 9 Hz, 4H), 7.77 (d, *J* = 9 Hz, 4H), 8.02 (s, 2H).

^{13}C NMR (D_2O, 75 MHz) δ: 36.9, 40.3, 54.4, 120.9, 122.3, 127.5, 142.5, 147.6, 148.7, 170.4.

IR (KBr): 3334 (br), 2965, 2931, 1663, 1599, 1526, 1368 cm^{-1}.

HRMS: calculated for $C_{24}H_{27}N_{12}O_6S_2$ m/z 643.1618; found 643.1614.

Preparation of 5b

To L-Cystine (2 g, 8.33 mmol) in 100 mL methanol, dry HCl (g) was bubbled over a period of 7 h. The reaction mixture was subjected to high vacuum and dried well. The dimethyl ester hydrochloride obtained was dissolved in ethyl acetate and washed with 50 mL of 10% aq. Na_2CO_3 solution. The organic layer was dried over Na_2SO_4 and evaporated to yield 1.5 g of **5b**.

Yield: 67 %

m.p : 136-138 °C

^{1}H NMR ($CDCl_3$+D_2O, 300 MHz) δ: 3.13 (m, 4H), 3.78 (s, 6H), 4.37 (br s, 2H).

IR (KBr) : 3368 (br), 1748, 1682 cm^{-1}

Preparation of 6

To an ice cooled solution of **5b** (500 mg, 1.8 mmol) in dry chloroform, triethylamine (0.5 mL, 4.1 mmol) was added. To this well-stirred solution, Di-*tert*-butyl dicarbonate (893 mg, 4.1 mmol) was added drop-wise over a period of 2 h. After stirring for 12 h, the reaction mixture was washed sequentially with 0.2 N H_2SO_4, and water. The organic layer was dried over Na_2SO_4 and evaporated to yield 800 mg of the product.

Yield : 94 %

m.p : 92-94 °C

^{1}HNMR ($CDCl_3$, 300 MHz) δ: 1.22 (s, 18H), 3.21 (br s, 4H), 3.77 (s, 6H), 4.84 (m, 2H), 6.52 (d, *J* = Hz, 2H).

^{13}C NMR ($CDCl_3$, 75 MHz) δ: 28.7, 40.4, 51.6, 56.6, 80.1, 155.3, 171.0.

IR (KBr) : 3298 (br), 2973, 1750, 1643, 1534, 1435 cm^{-1}.

HRMS calculated for $C_{18}H_{32}N_2O_8S_2Na$, m/z 491.1498, found 491.1519.

Dynamic Light Scattering (DLS):

Solutions were prepared by dissolving 10 mg of Ag NPs in water followed by filtration using Nylon syringe filter (13 mm / 0.2 μm) and was used for the measurement. The particle size distribution was measured by Malvern Zetasizer ZS90 DLS spectrometer with 633 nm CW laser.

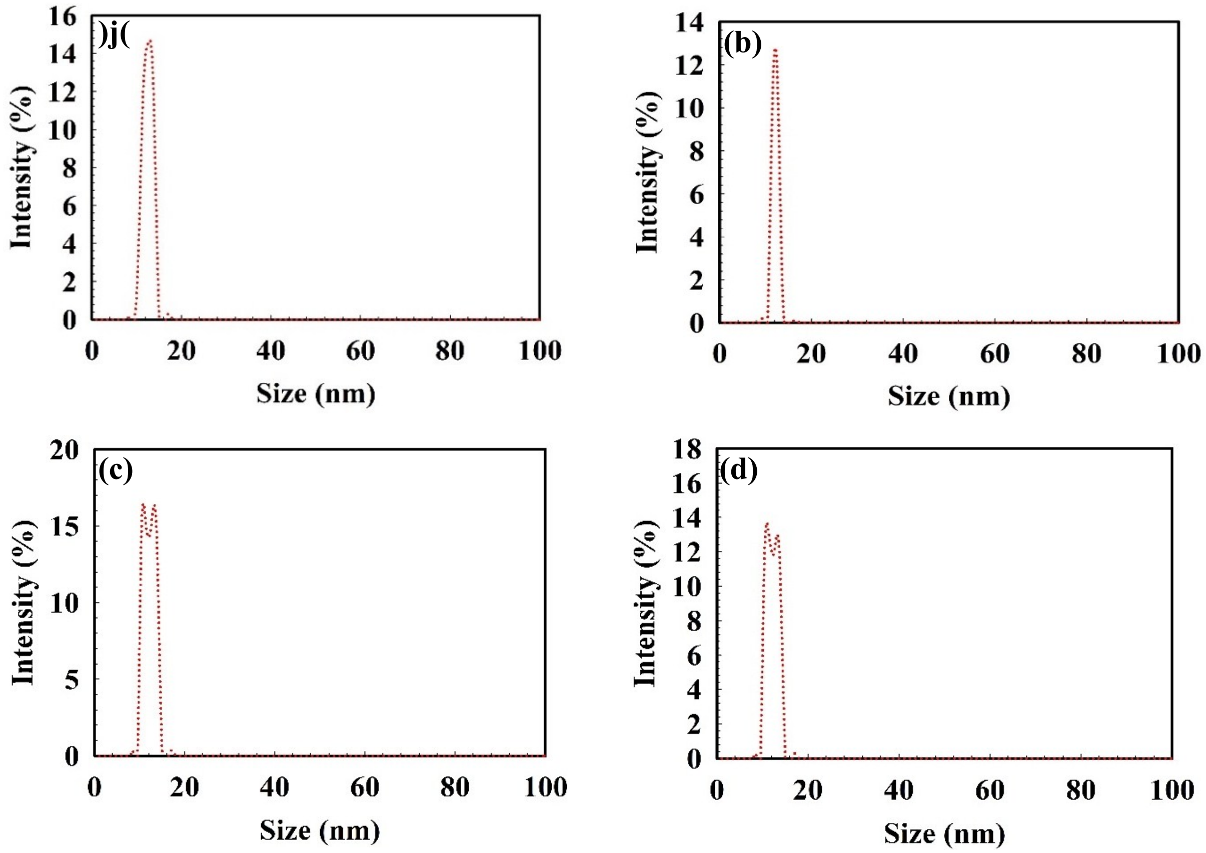

Fig. S1 DLS profiles for the Ag NPs (a) **3a**-Ag NPs (b) **3b**-Ag NPs (c) **5b**-Ag NPs (d) **6**-Ag NPs dispersed in water.

Table S1. The size of the Ag NPs prepared from various cysteine-based molecules. The average size has been calculated using image J software for 45 particles

Type of Ag NPs	Average particle size
3a-Ag NPs	11.87 nm
3b-Ag NPs	11.27 nm
5b-Ag NPs	12.01 nm
6-Ag NPs	13.01 nm

Energy dispersive X-ray analysis (EDX)

Ag NPs were dried well and mounted on carbon tape attached to a stub. EDX-SEM experiments were performed by ZEISS EVO®18 instrument with an EHT of 20 kV.

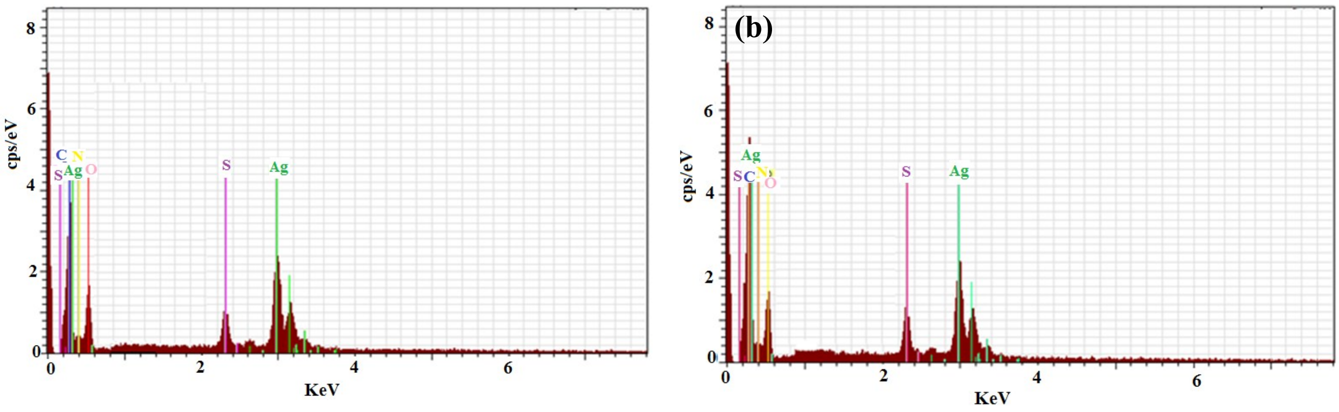

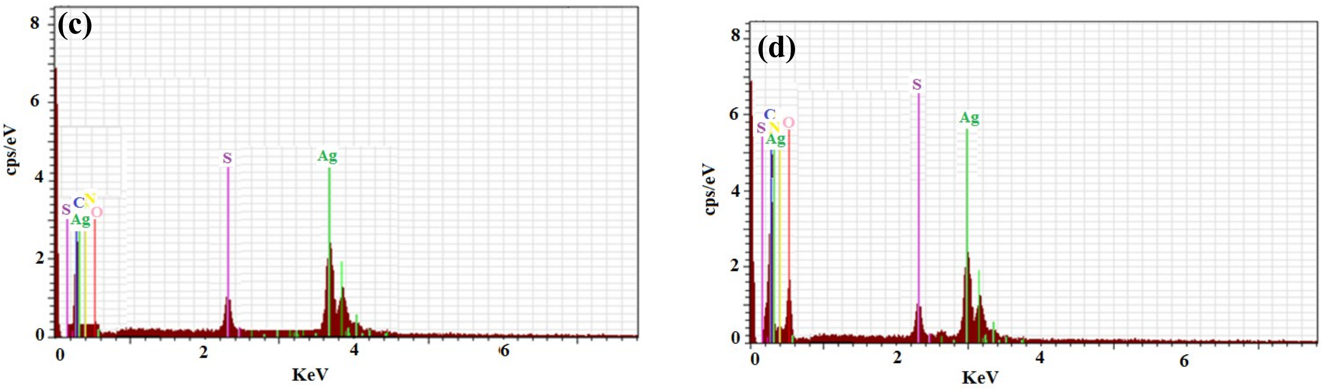

Fig. S2 EDX profiles for the Ag NPs (a) **3a**-Ag NPs (b) **3b**-Ag NPs (c) **5b**-Ag NPs (d) **6**-Ag NPs.

pH measurement studies

The stability of the Ag NPs at different pH were measured by UV-visible spectroscopic studies by monitoring the changes in the absorption maxima. The pH of solutions were varied by adding either 10 mM HCl/NaOH to the Ag NPs solution and pH were measured by a pH meter.

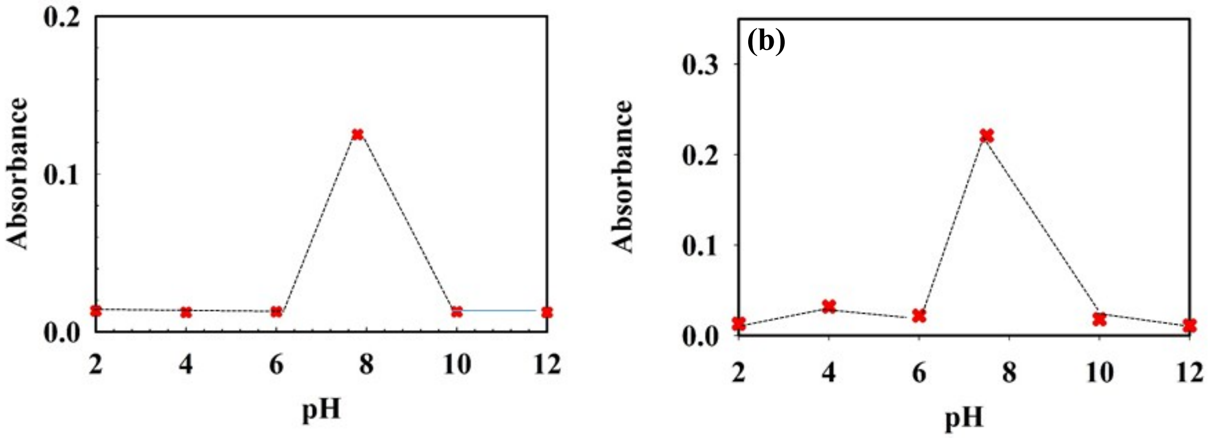

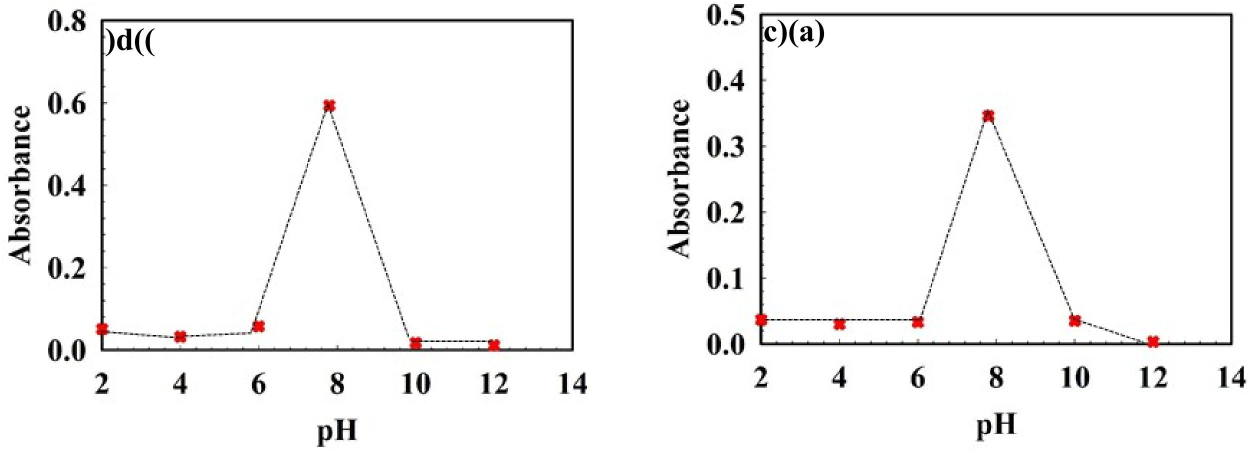

Fig. S3 UV-visible spectra for Ag NPs at different pH conditions (a) **3a**-Ag NPs (b) **3b**-Ag NPs (c) **5b**-Ag NPs (d) **6**-Ag NPs.

Competitive experiment studies with anions

The interference of various anion salts on the sensing ability of Ag NPs was studied by UV-visible spectroscopic method by monitoring the changes in SPR bands at 430 nm. All the anion salt solutions were prepared in water.

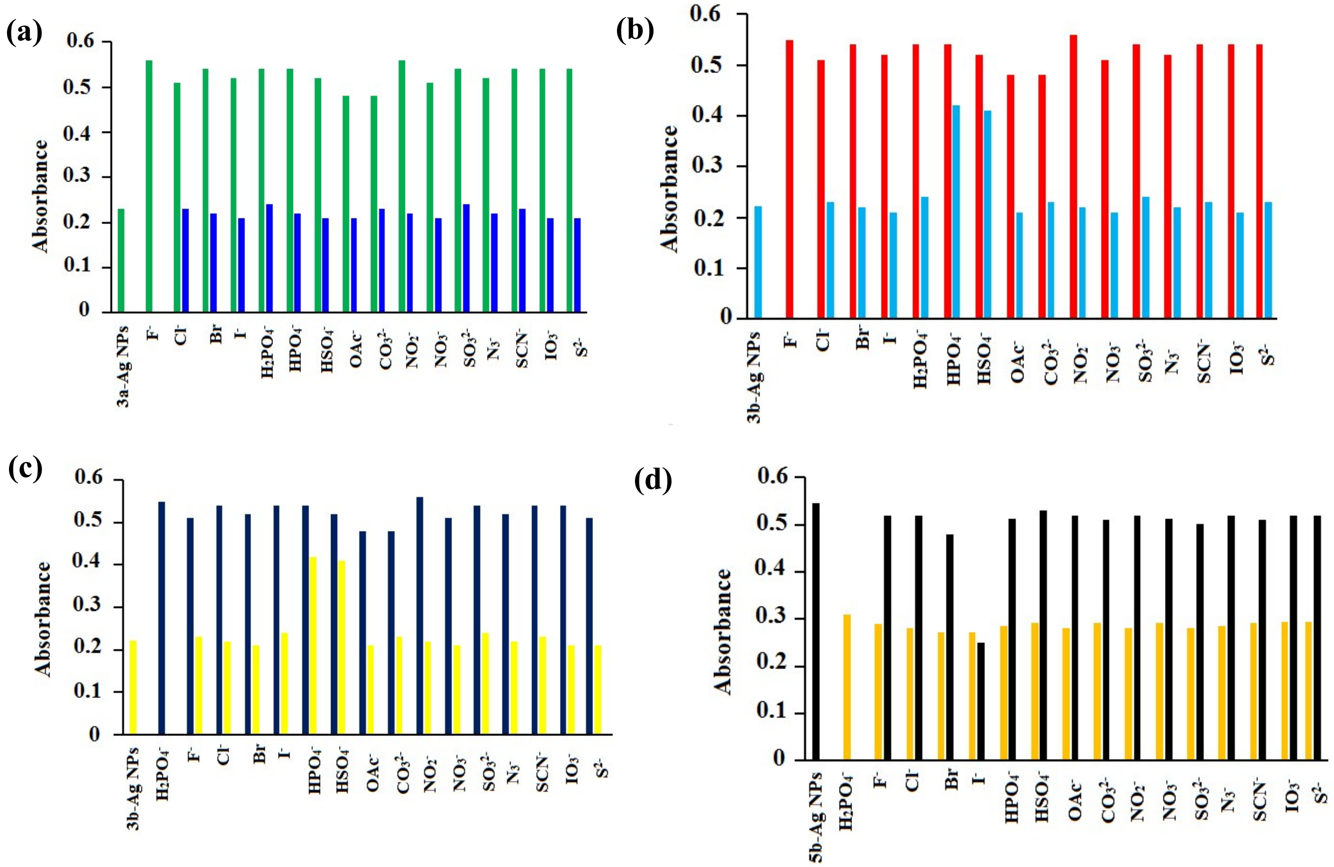

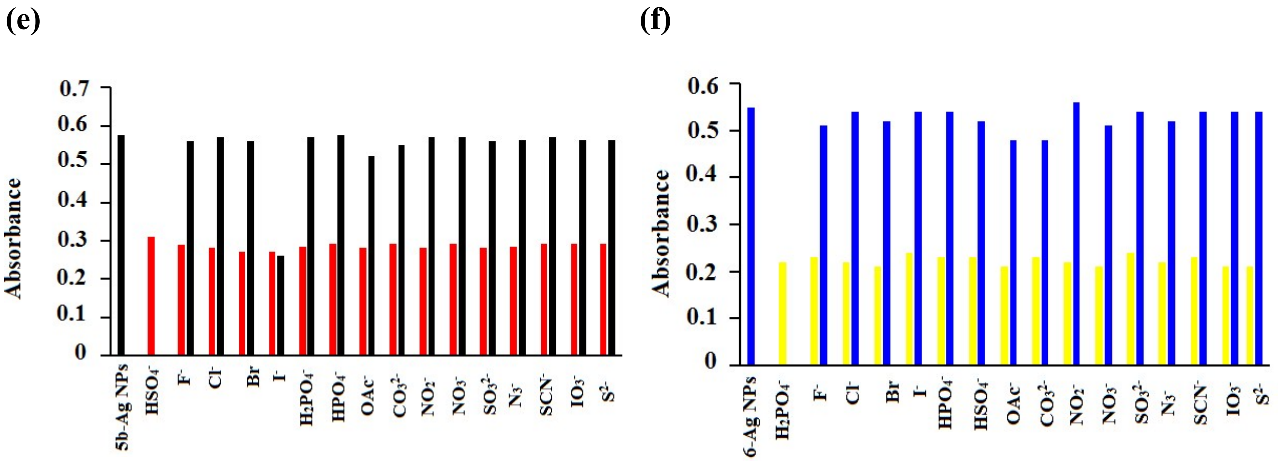

Fig. S4 (a) Selectivity studies of **3a**-Ag NPs for F^- (2 μM) in the presence of other anions (100 μM). Green bars indicate **3a**-Ag NPs + F^- + other anions and blue bars indicate **3a**-Ag NPs + other anions. (b) Selectivity studies of **3b**-Ag NPs for F^- (2.8 μM) in the presence of other anions (100 μM). Red bars indicate **3a**-Ag NPs + F^- + other anions and blue bars indicate **3b**-Ag NPs + other anions. (c) Selectivity studies of **3b**-Ag NPs for $H_2PO_4^-$ (2.4 μM) in the presence of other anions (100 μM). Blue bars indicate **3b**-Ag NPs + $H_2PO_4^-$ + other anions and yellow bars indicate **3b**-Ag NPs + other anions. (d) Selectivity studies of **5b**-Ag NPs for $H_2PO_4^-$ (3.8 μM) in the presence of other anions (100 μM). Yellow bars indicate **5b**-Ag NPs + $H_2PO_4^-$ + other anions and black bars indicate **5b**-Ag NPs + other anions. (e) Selectivity studies of **5b**-Ag NPs for HSO_4^- (2.1 μM) in the presence of other anions (100 μM). Red bars indicate **3b**-Ag NPs + HSO_4^- + other anions and black bars indicate **3b**-Ag NPs + other anions. (f) Selectivity studies of **6**-Ag NPs for $H_2PO_4^-$ (2.8 μM) in the presence of other anions (100 μM). Yellow bars indicate **6**-Ag NPs + $H_2PO_4^-$ + other anions and blue bars indicate **6**-Ag NPs + other anions

Limit of detection (LOD) of Ag NPs with analytes

A linear correlation exists between A_{430}/A_0 and the concentration of C of the analyte over the tested concentration range. The plot of concentration against A_{430}/A_0 gives a straight line with a linear equation $A_{430}/A_0 = mx + C$. The term x stands for the LOD which can be calculated from the linear equation.

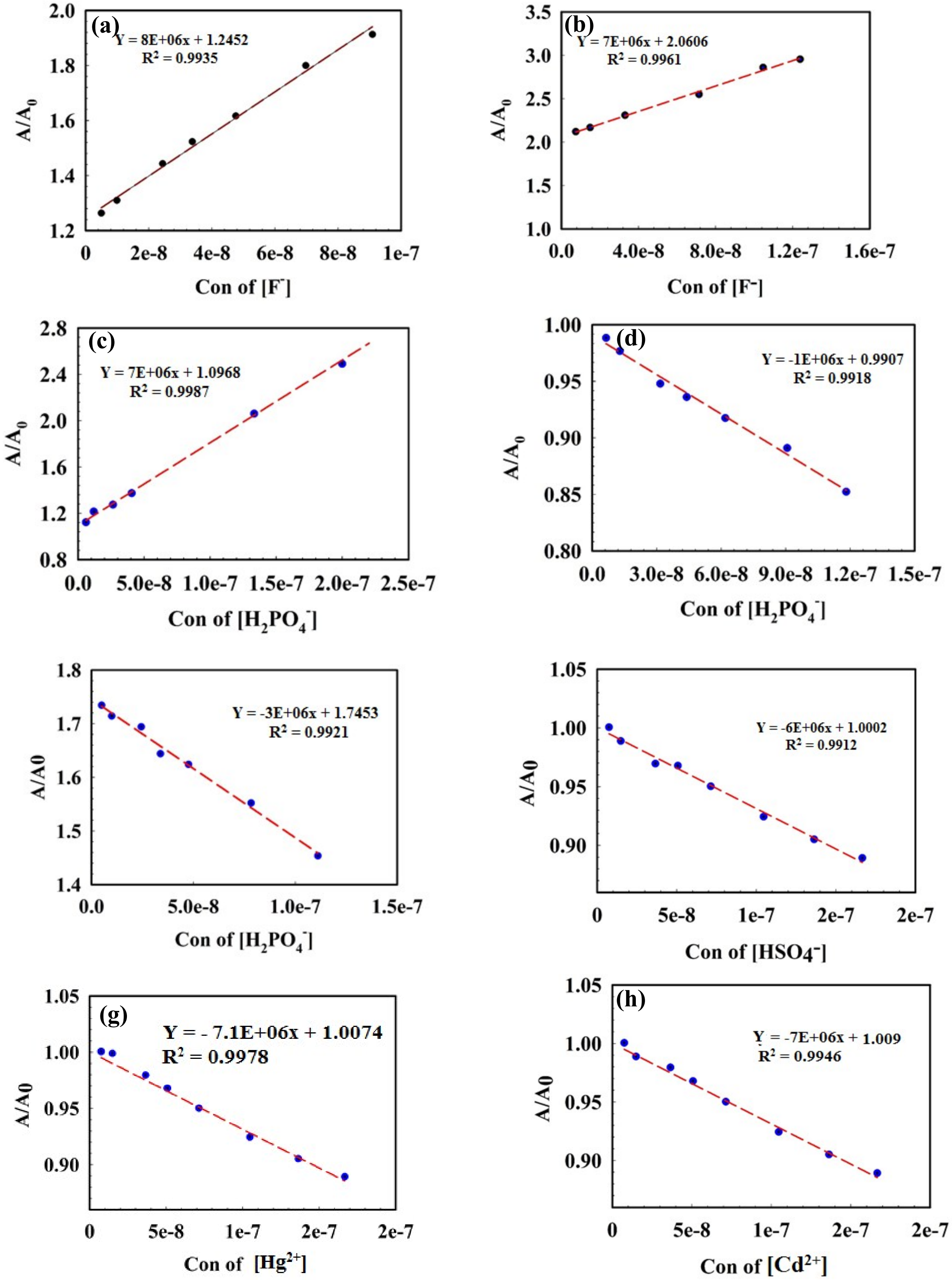
(a)
Y = 8E+06x + 1.2452
R^2 = 0.9935
A/A_0
2.0
1.8
1.6
1.4
1.2
0
2e-8
4e-8
6e-8
8e-8
1e-7
Con of [F^-]
(b)
Y = 7E+06x + 2.0606
R^2 = 0.9961
A/A_0
3.5
3.0
2.5
2.0
1.5
1.0
0.0
4.0e-8
8.0e-8
1.2e-7
1.6e-7
Con of [F^-]
(c)
Y = 7E+06x + 1.0968
R^2 = 0.9987
A/A_0
2.8
2.4
2.0
1.6
1.2
0.8
0.0
5.0e-8
1.0e-7
1.5e-7
2.0e-7
2.5e-7
Con of [$H_2PO_4^-$]
(d)
Y = -1E+06x + 0.9907
R^2 = 0.9918
A/A_0
1.00
0.95
0.90
0.85
0.80
0.0
3.0e-8
6.0e-8
9.0e-8
1.2e-7
1.5e-7
Con of [$H_2PO_4^-$]
Y = -3E+06x + 1.7453
R^2 = 0.9921
A/A0
1.8
1.7
1.6
1.5
1.4
0.0
5.0e-8
1.0e-7
1.5e-7
Con of [$H_2PO_4^-$]
Y = -6E+06x + 1.0002
R^2 = 0.9912
A/A0
1.05
1.00
0.95
0.90
0
5e-8
1e-7
2e-7
2e-7
Con of [HSO4⁻]
(g)
Y = - 7.1E+06x + 1.0074
R^2 = 0.9978
A/A0
1.05
1.00
0.95
0.90
0
5e-8
1e-7
2e-7
2e-7
Con of [Hg^{2+}]
(h)
Y = -7E+06x + 1.009
R^2 = 0.9946
A/A0
1.05
1.00
0.95
0.90
0
5e-8
1e-7
2e-7
2e-7
Con of [Cd^{2+}]

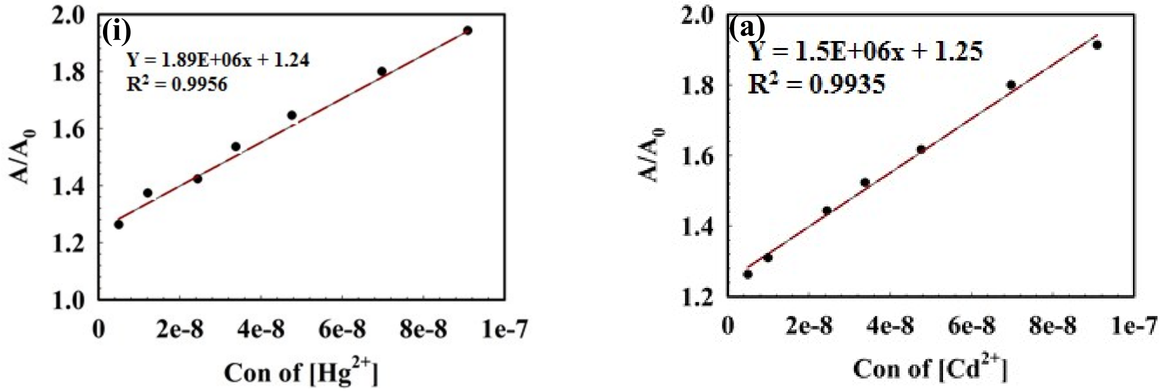

Fig. S5 Determination of LOD of Ag NPs with analytes (a) **3a**-Ag NPs with F^- (b) **3b**-Ag NPs with F^- (c) **3b**-Ag NPs with $H_2PO_4^-$ (d) **5b**-Ag NPs with $H_2PO_4^-$ (e) **5b**-Ag NPs with HSO_4^- (f) **6-**Ag NPs with $H_2PO_4^-$ (g) **3a-**Ag NPs with Hg^{2+} (h) **3a-**Ag NPs with Cd^{2+} (i) **3b-**Ag NPs with Hg^{2+} (i) **3b-**Ag NPs with Cd^{2+}

^{1}H NMR analysis of 3b-Ag NPs

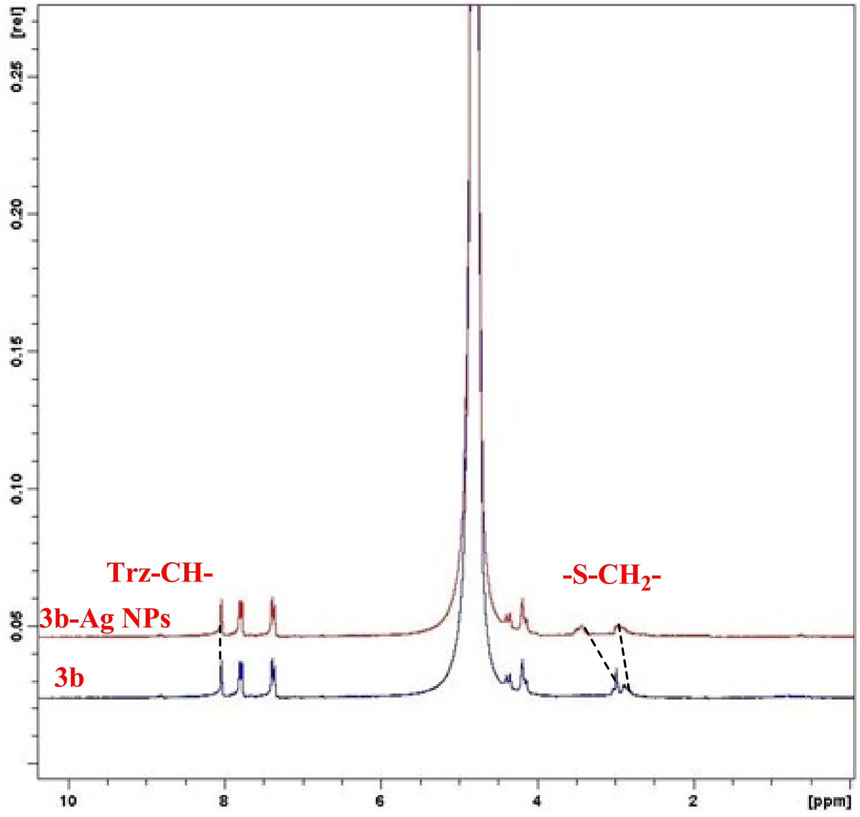

Fig. S6 ^{1}H-NMR spectra of **3b** and **3b-**Ag NPs in D_2O (300 MHz).

Competitive experiment studies with cations

The interference of various cation salts on the sensing ability of Ag NPs was studied by UV-visible spectroscopic method by monitoring the changes in SPR bands. All the cation salt solutions were prepared in water.

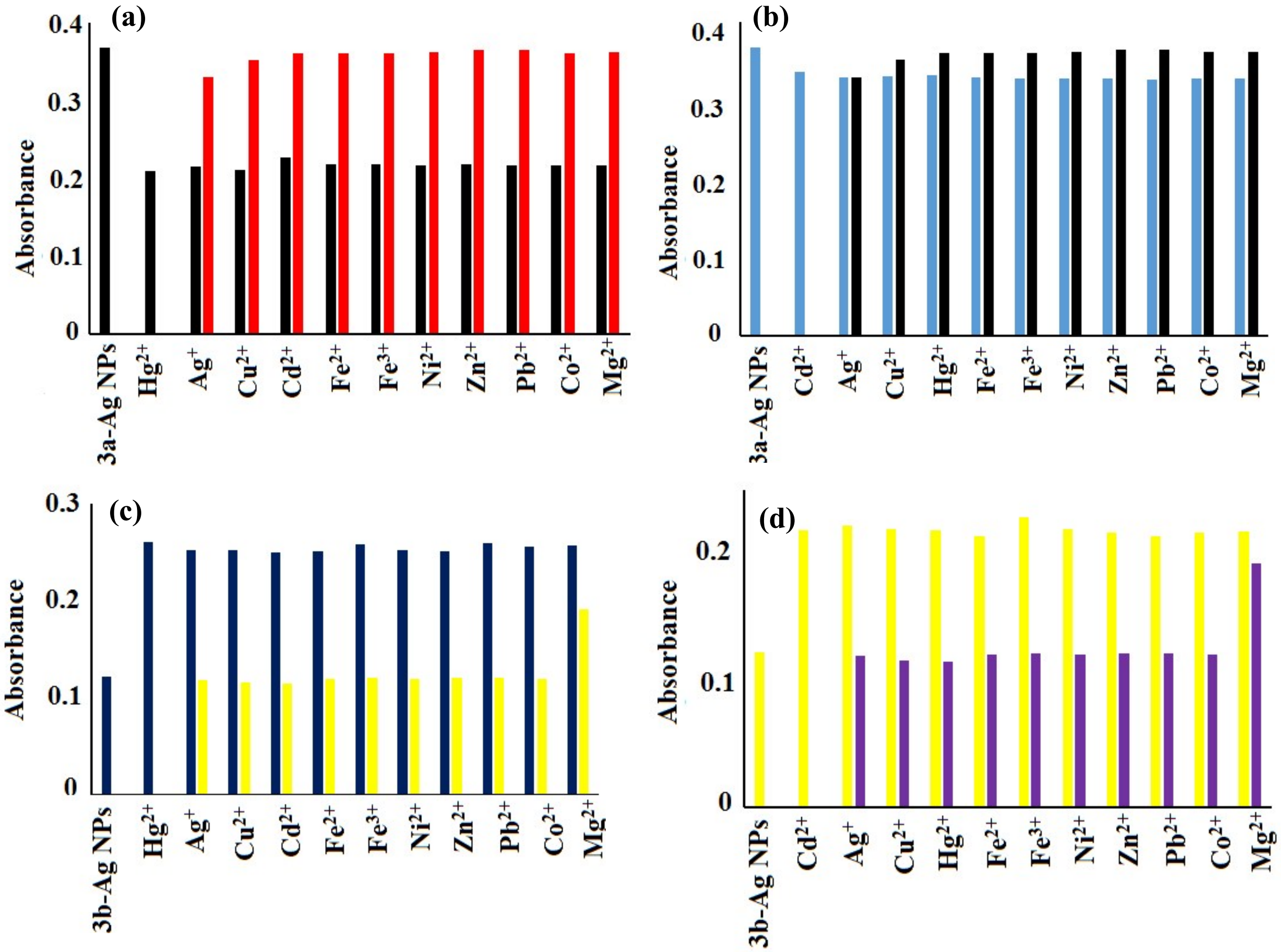

Fig. S7 (a) Selectivity studies of **3a**-Ag NPs for Hg^{2+} (3 μM) in the presence of other anions (100 μM). Black bars indicate **3a**-Ag NPs + Hg^{2+} + other cations and red bars indicate **3a**-Ag NPs + other cations. (b) Selectivity studies of **3a**-Ag NPs for Cd^{2+} (4.2 μM) in the presence of other anions (100 μM). Blue bars indicate **3a**-Ag NPs + Cd^{2+} + other cations and blue bars indicate **3b**-Ag NPs + other cations. (c) Selectivity studies of **3b**-Ag NPs for Hg^{2+} (3 μM) in the presence of other cations (100 μM). Blue bars indicate **3b**-Ag NPs + Hg^{2+} + other anions and yellow bars indicate **3b**-Ag NPs + other cations. (d) Selectivity studies of **3b**-Ag NPs for Cd^{2+} (4.2 μM) in the presence of other cations (100 μM). Yellow bars indicate **3b**-Ag NPs + Cd^{2+} + other anions and purple bars indicate **3b**-Ag NPs + other cations.

HR-TEM measurements for the aggregation of Ag NPs with metal ions

Samples for HR-TEM were prepared by dissolving the compound in water by sonication. Metal salts; $Hg(ClO_4)_2$ and $Cd(ClO_4)_2$ (10 μM) were also dissolved in water and admixed with the Ag NPs solution A 2μl aliquot of the sample solution was placed on a 200 mesh copper grid and the excess water was removed using a filter paper and samples were viewed using a TECHNAI G2 (20STWIN) electron microscope.

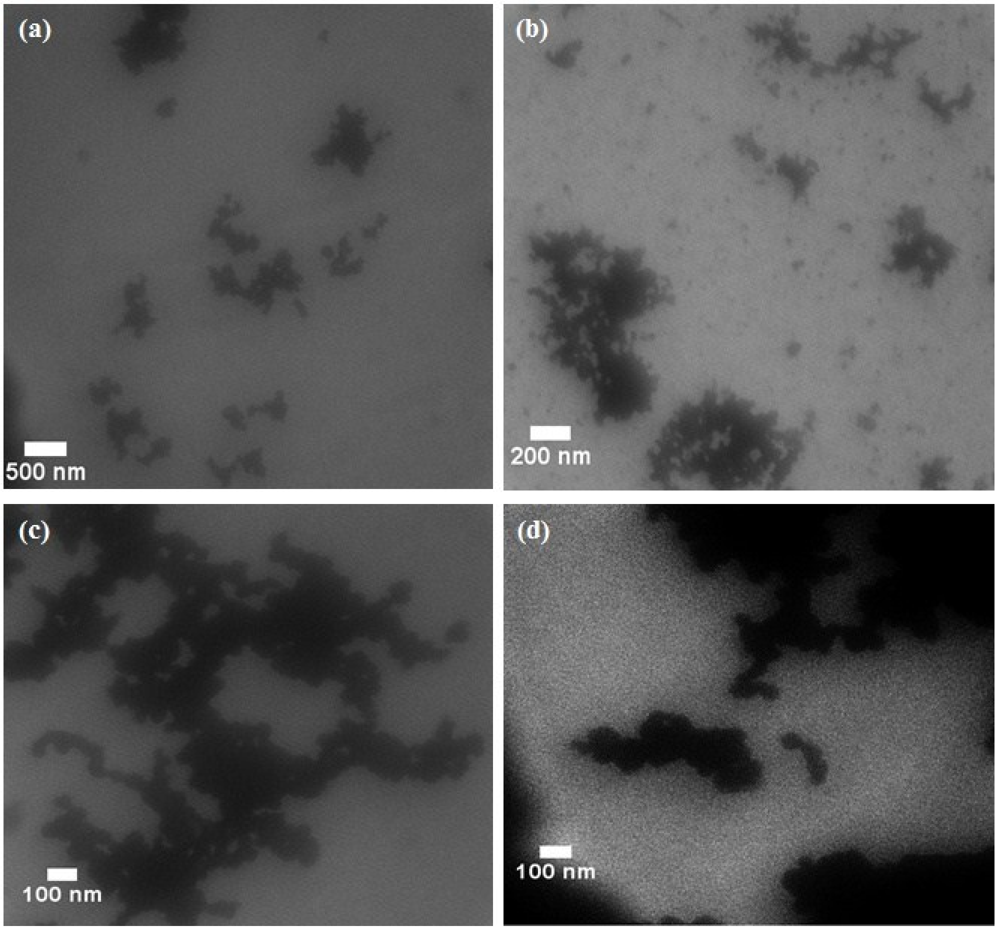

Fig. S8 HR-TEM measurements for (a) **3a**-Ag NPs with Hg^{2+} (b) **3a**-Ag NPs with Cd^{2+} (c) **3b**-Ag NPs with Hg^{2+} (d) **3b**-Ag NPs with Cd^{2+} . $[C_M{}^{2+}]$: $1x10^{-9}$ M.

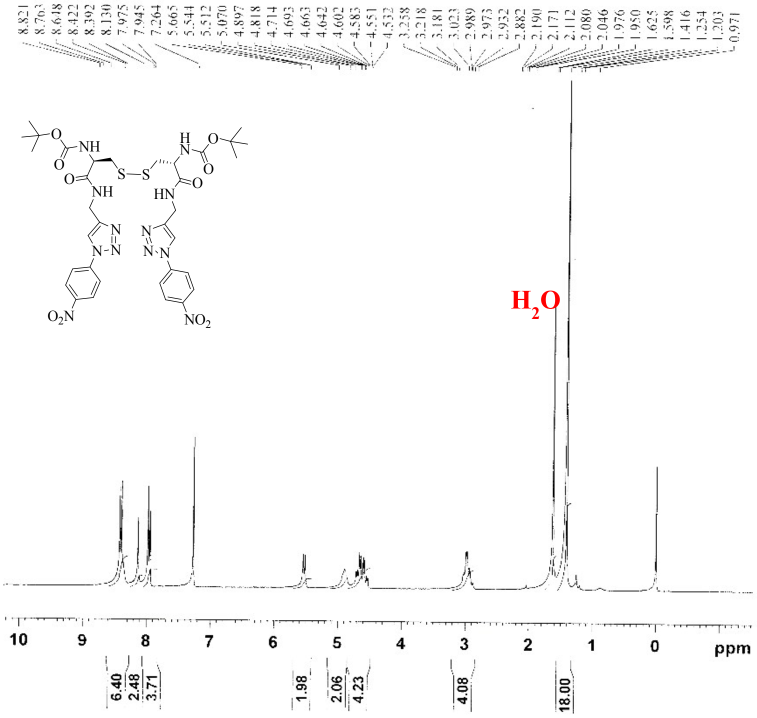

Fig. S9 ^{1}H-NMR spectrum of **3a** ($CDCl_3$, 300 MHz).

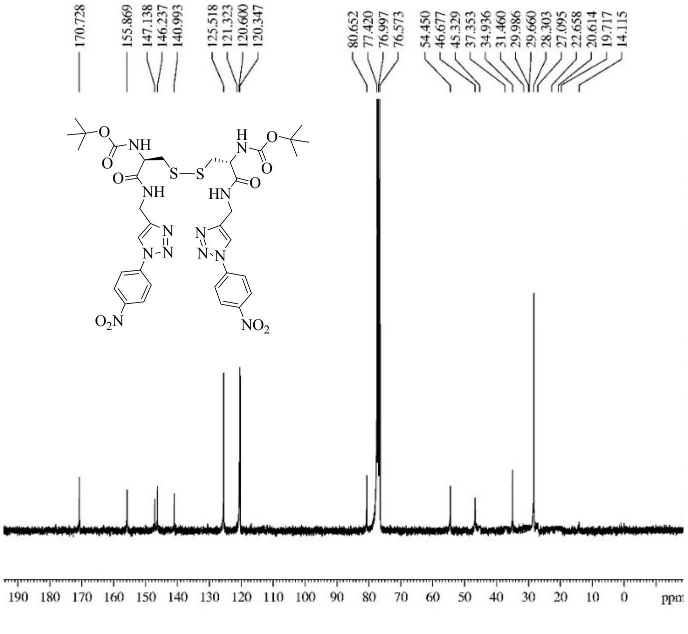

Fig. S10 ^{13}C-NMR spectrum of **3a** ($CDCl_3$, 75 MHz).

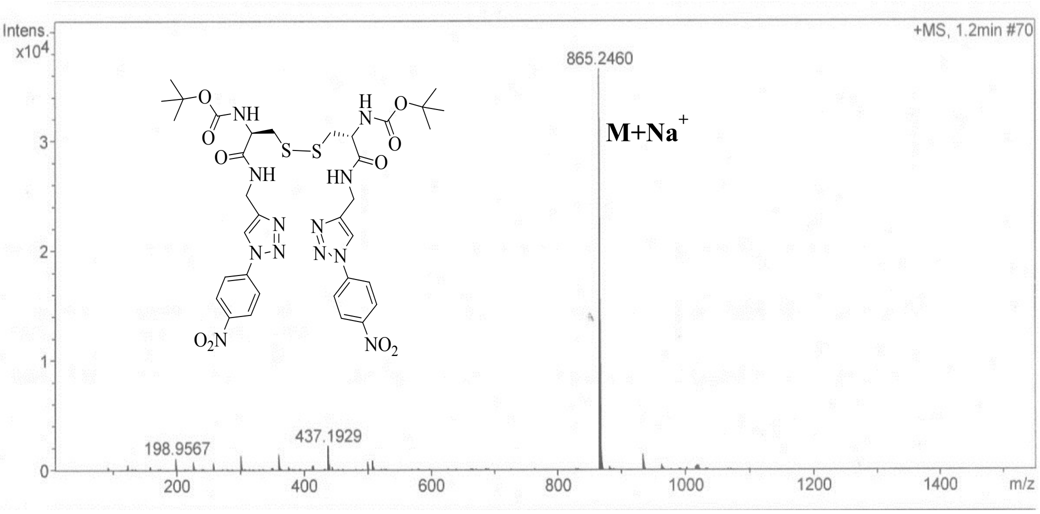

Fig. S11 ESI-Mass spectrum of **3a**

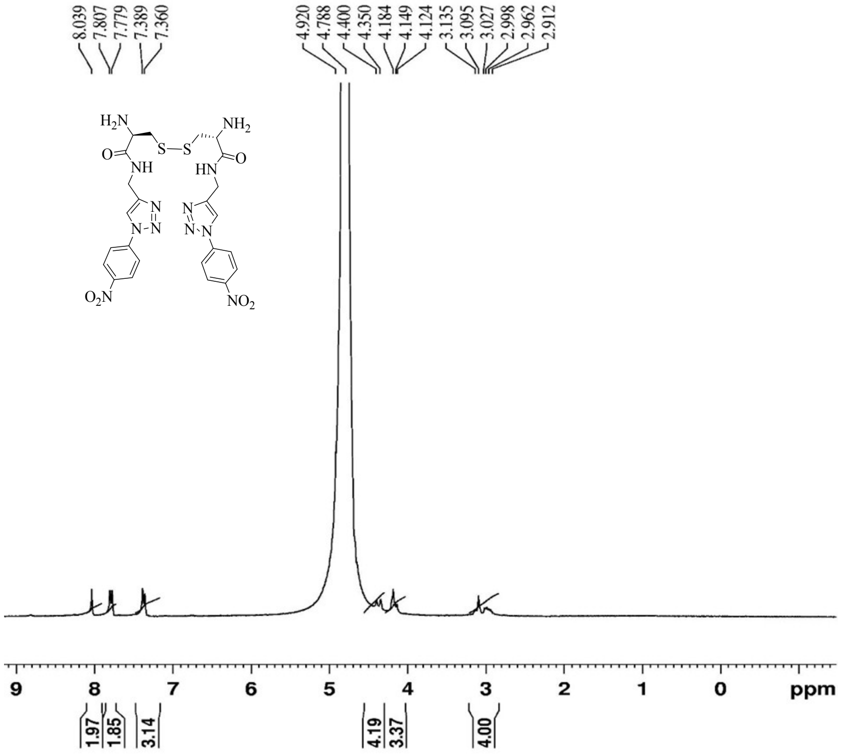

Fig.S12 ^{1}H-NMR spectrum of **3b** (D$_2$O, 300 MHz)

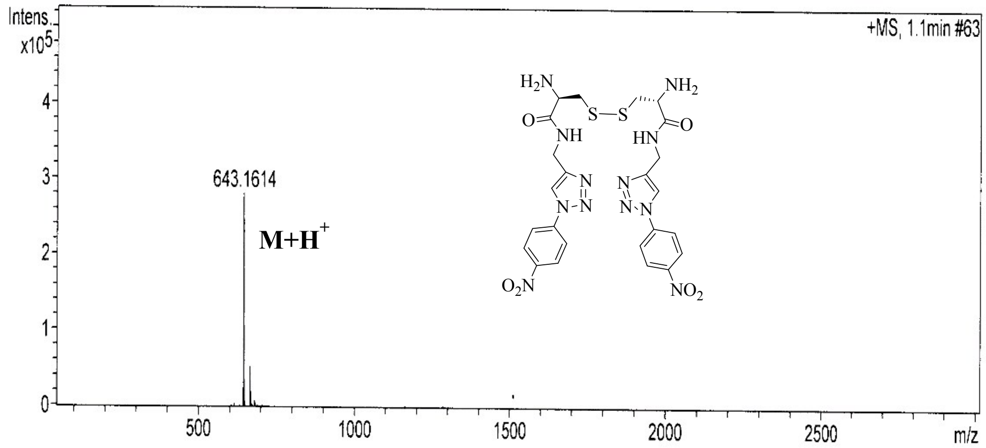

Fig. S13 ESI-Mass spectrum of **3b**

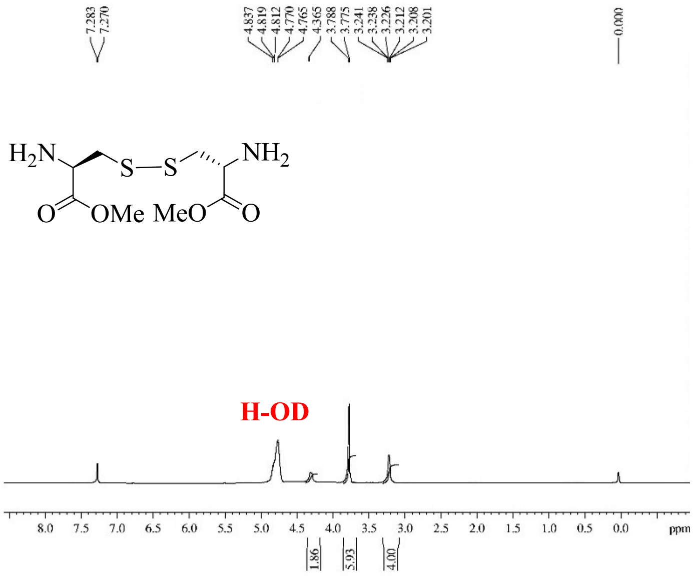

Fig. S14 ^{1}H-NMR spectrum ofr **5b** ($CDCl_3$ + D_2O, 300 MHz)

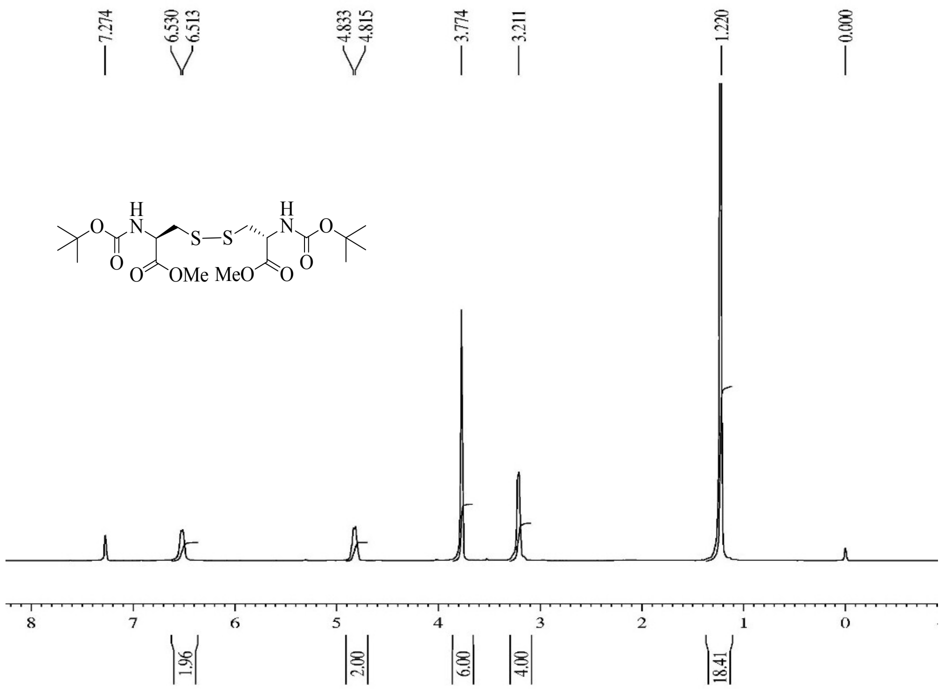

Fig. S15 ^{1}H-NMR spectrum of **6** ($CDCl_3$, 300 MHz)

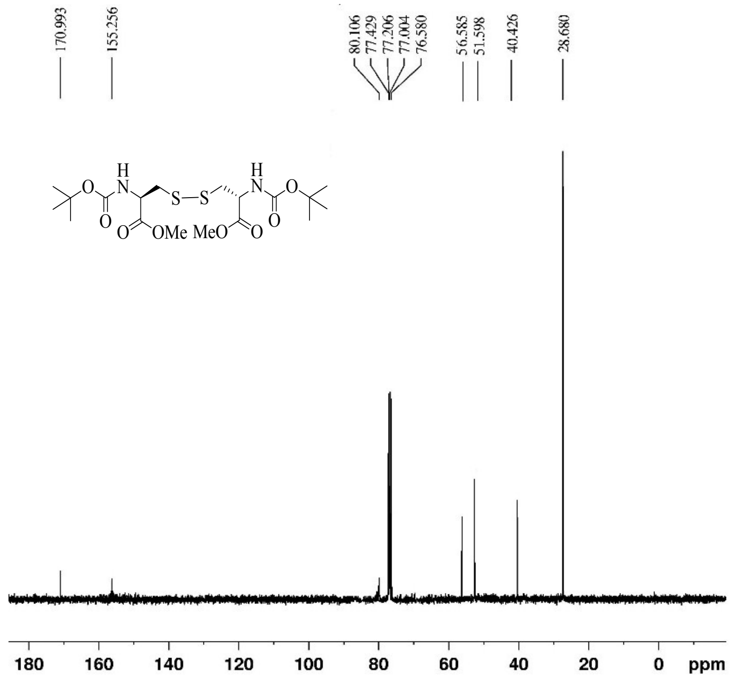

Fig. S16 ^{13}C-NMR spectrum of **6** ($CDCl_3$, 75 MHz)

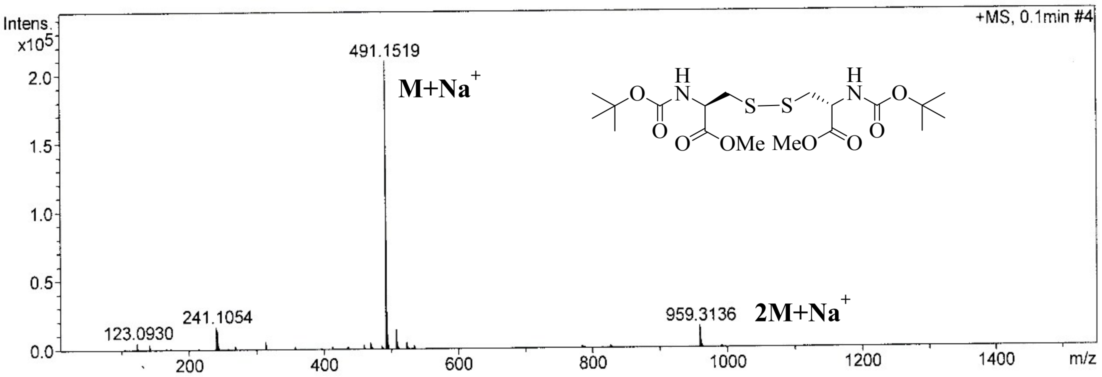

Fig. S17 ESI-Mass spectrum of **6**